Analysis of slender reinforced concrete frames

PDF erstellt am: **11.09.2024**

Analysis of Slender Reinforced Concrete Frames

Calcul des cadres en béton armé selon la théorie du 2e ordre

Berechnung von Stahlbetonrahmen nach der Theorie 2. Ordnung

K. AAS-JAKOBSEN
Dr. sc. techn., formerly, research associate

M. GRENACHER
Research associate

Institute of Structural Engineering, Swiss Federal Institute of Technology (ETH), Zurich (Switzerland)

1. Introduction

This paper outlines a method to determine the maximum load carrying capacity of a plane frame with given cross sections and reinforcements.

The present paper based on an investigation described in [1] differs from other investigations [2], [3], [4], [5], [6], [7], [8] in three respects:

— The frame can have an arbitrary geometry.

— An arbitrary load history can be followed.

— A displacement controlled procedure is used which allows the determination of unstable configurations of the frame.

The two main difficulties in the analysis of slender reinforced concrete frames are due to

— the influence of the displacements on the equilibrium of the frame, producing a "geometrical" non-linearity;

— the non-linear stress-strain-time relations for the materials causing a "material" non-linearity.

The two non-linearities are treated separately as shown schematically in Fig. 1. The geometrical non-linearity is considered in a second order elastic analysis. Given are loads P, bending rigidities EI and axial rigidities EA for all elements of the frame. The moment M, the axial force N and the corresponding strain distribution for all sections are determined. The strain
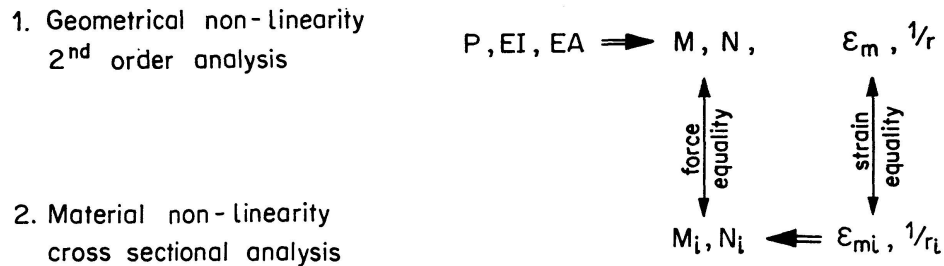
Fig. 1. Schematic illustration of the analysis.

distribution is given by two parameters. Herein, the middle strain ϵ_m in the reference axis of the members and the curvature $1/r$ are used.

The material non-linearity is taken into account in the cross sectional analysis. Given are cross section, reinforcement, stress-strain-time relation for the materials and a strain distribution (ϵ_{mi}, $1/r_i$). The subscript "i" is used for reference to the cross sectional analysis. The moment M_i and axial force N_i are determined.

The elastic and the cross sectional analysis are coupled together by the requirement of equality of the determined forces in the elastic and the cross sectional analysis. Similarly, equality of the strains determined in the elastic analysis and of the strains assumed in the cross sectional analysis must be satisfied.

The critical load of the structure corresponds to the peak on a load-deflection curve separating the stable from the unstable equilibrium configuration. In this range a deformation controlled procedure must be used to assure convergence. Hence, the deformation at some point of the structure is increased by steps to obtain the load-displacement response.

2. Second Order Elastic Analysis

The elastic frame analysis is performed by means of the finite element method. A frame may be visualized as an assemblage of elements interconnected at their ends which are referred to as nodal points or nodes. If the force-displacement relations for each element are known, the equilibrium configuration of the complete structure can be expressed in terms of the nodal
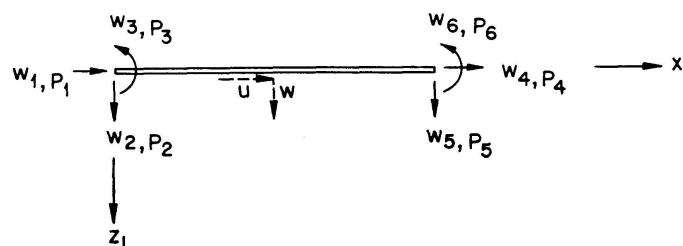

Fig. 2. Element in local coordinates.

displacements. The force-displacement relationship for the element shown in Fig. 2 can be written as

$$[K]\{w\} = \{P\},\tag{1}$$

in which $\{w\}$ is the displacement vector of the element and $\{P\}$ the corresponding force vector:

$$\{w\} = \begin{Bmatrix} w_1 \\ w_2 \\ w_3 \\ w_4 \\ w_5 \\ w_6 \end{Bmatrix}, \qquad \{P\} = \begin{Bmatrix} P_1 \\ P_2 \\ P_3 \\ P_4 \\ P_5 \\ P_6 \end{Bmatrix}.$$

Applying standard finite element techniques, the stiffness matrix $[K]$ can be written as

$$[K] = [K_1] + [K_2],$$

where $[K_1]$ is the first order stiffness matrix,

$\quad [K_2]$ is the non-linear geometrical stiffness matrix,

$\quad [K_1]$ and $[K_2]$ are given in Fig. 3.

If the element is inclined at an angle θ with the x-axis, as shown in Fig. 4, the given stiffness matrix above relates to the local coordinates $x_l - z_l$. The

Fig. 3. Local element stiffness matrix $[K]=[K_1]+[K_2]$.
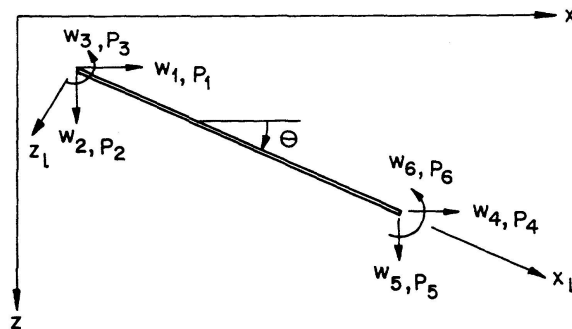

Fig. 4. Global forces and displacements.

global stiffness matrix $[K]$ in the x-z coordinate system is then given by

$$[K] = [R]^T [K_l] [R].$$

$[K_l]$ is the local stiffness matrix given in Fig. 3.

$[R]$ is the transformation matrix relating local displacements $\{w_l\}$ and global displacements $\{w\}$, or local loads $\{P_l\}$ and global loads $\{P\}$ as follows:

$$\{w_l\} = [R]\{w\}, \tag{2}$$

$$\{P_l\} = [R]\{P\},$$

$$[R] \quad \text{is given in Fig. 5.}$$

The global element stiffness matrix $[K] = [K_1] + [K_2]$ is given in Fig. 6.

$$[R] =
\begin{bmatrix}
C & S & & & & \\
-S & C & & & & \\
 & & 1 & & & \\
 & & & C & S & \\
 & & & -S & C & \\
 & & & & & 1
\end{bmatrix}$$

$$\{w_l\} = [R]\{w\}$$
$$\{P_l\} = [R]\{P\}$$

$$S = \sin\Theta$$
$$C = \cos\Theta$$

Fig. 5. Transformation matrix $[R]$.

$[K_1] =$

$\frac{EA}{l}C^2 + \frac{12EI}{l^3}S^2$	$\left(\frac{EA}{l} - 12\frac{EI}{l^3}\right)SC$	$-\frac{6EI}{l^2}S$	$-k_{11}$	$-k_{12}$	k_{13}
	$\frac{EA}{l}S^2 + \frac{12EI}{l^3}C^2$	$\frac{6EI}{l^2}C$	$-k_{12}$	$-k_{22}$	k_{23}
		$4\frac{EI}{l}$	$-k_{13}$	$-k_{23}$	$\frac{2EI}{l}$
	symmetric		k_{11}	k_{12}	$-k_{13}$
				k_{22}	$-k_{23}$
					k_{33}

$[K_2] = N$

$\frac{6}{5 \cdot l}S^2$	$-\frac{6}{5l}SC$	$-\frac{1}{10}S$	$-k_{11}$	$-k_{12}$	k_{13}
	$\frac{6}{5l}C^2$	$\frac{1}{10}C$	$-k_{12}$	$-k_{22}$	k_{23}
		$\frac{2l}{15}$	$-k_{13}$	$-k_{23}$	$-\frac{l}{30}$
	symmetric		k_{11}	k_{12}	$-k_{13}$
				k_{22}	$-k_{23}$
					k_{33}

$S = \sin\Theta$ $C = \cos\Theta$

Fig. 6. Global element stiffness matrix $[K] = [K_1] + [K_2]$.

Similar to the force-displacement relationship for the element the force-displacement relationship for the complete structure, or the complete system of elements, can be written as

$$[K]\{w\} = \{P\},$$ (3)

in which $\{w\}$ now contains all nodal displacements and $\{P\}$ all nodal loads.

The system stiffness matrix for the complete structure is obtained by superposition of the individual element stiffness matrices.

When the system stiffness matrix $[K]$ and the load matrix $\{P\}$ have been established, the system of equations is adjusted according to the given boundary conditions. If some displacement, for instance w_j, is identical to zero, this can be taken into account in a simple manner by replacing the diagonal stiffness coefficient K_{jj} by a large number, say 10^{50}.

The solution of the linear system of equations, Eq. (3) is most efficiently carried out taking into account the symmetry and the banded structure of the system stiffness matrix.

It should be noted that the axial force N must be known in order to evaluate the element matrix $[K_2]$ in Fig. 6. The axial force is usually not known in advance, and an iterative procedure must be used. In the first cycle N is chosen equal to zero and the first order forces are calculated. In the second cycle the axial forces found in the first cycle are used.

Usually the axial forces are practically not influenced by the second order effects, such that two cycles are generally sufficient.

When the displacements have been determined, the element forces are found by substituting $\{w\}$ back into Eq. (1). It should be noted that $[K]$ in Eq. (1) is the local element stiffness matrix given in Fig. 3. The global displacements are transformed into local displacements according to Eq. (2).

3. Cross Sectional Analysis

In the cross sectional analysis each section is divided into narrow strips which are assumed to behave as concentrically loaded fibers.
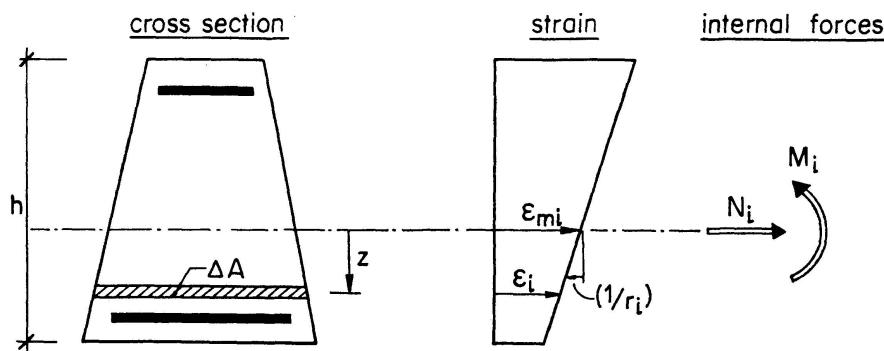

Fig. 7. Cross section, strain distribution and forces.

The resultant forces M_i and N_i are given by (Fig. 7)

$$M_i = \sum \sigma z \varDelta A,$$
$$N_i = \sum \sigma \varDelta A. \tag{4}$$

The strain ϵ, positive when in tension, is assumed to be linearly distributed over the section. Then

$$\epsilon_i = \epsilon_{mi} - \left(\frac{1}{r_i}\right) z, \tag{5}$$

where ϵ_{mi} is the axial strain in the reference axis,

$\left(\dfrac{1}{r_i}\right)$ is the curvature,

z is the distance from the axis.

The assumed stress-strain relationship for a virgin concrete specimen (previously not loaded) under instantaneous loading up to failure is shown in Fig. 8. For instantaneous unloading or reloading a linear relation between stress and strain is assumed both for steel and concrete:

$$\sigma = E\,(\epsilon_i - \epsilon_c - \epsilon_p), \tag{6}$$

where σ is the stress in the considered strip,

E is the "elastic" modulus for the material,

ϵ_i is the total strain,

ϵ_c is the "plastic" strain in the strip from the previous load history,

ϵ_p is the initial strain in the strip, for instance due to prestressing.

The "plastic" strain ϵ_c is due to yielding, creep and shrinkage. At a given time, the magnitude of the plastic strain can be determined from Eq. (6):

$$\epsilon_c = \epsilon - \sigma/E - \epsilon_p. \tag{7}$$

Steel is assumed to be elasto-plastic as shown in Fig. 8. Thus, the stress given by Eq. (6) is limited by the yield stress f_s.

The concrete stress determined from Eq. (6) is assumed to be limited by the stress-strain relationship for a virgin concrete under instantaneous loading. Hence, the stress-strain relationship for a virgin specimen is the envelope curve for the concrete stress-strain relations. The concrete is assumed to have no tensile strength. Concrete shows a time-dependent increase of the plastic strain ϵ_{cc} due to shrinkage and creep.

At a constant sustained stress the plastic strain due to creep is assumed to be given by

$$\epsilon_{cc} = \epsilon_0 \varphi, \tag{8}$$

$$\varphi = \varphi_\infty \frac{t}{T+t}, \tag{9}$$

where φ_∞ is the limiting creep factor,

T is the elapsed time until half the limiting creep is reached,

ϵ_0 is the short-time strain given by:

$$\epsilon_0 = -0.002\left(1 - \sqrt{1 + \frac{\sigma_c}{f_c}}\right). \tag{10}$$

The hyperbolic expression in Eq. (9) has been used in a number of investigations and seems to be in reasonable agreement with experimental data.

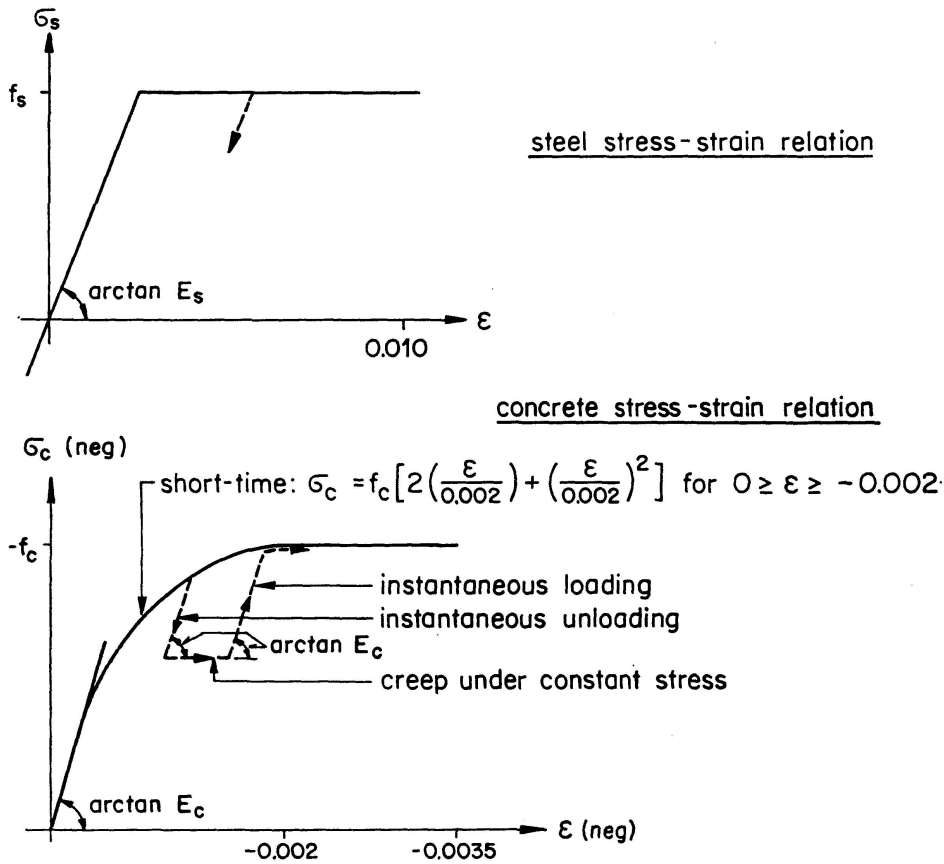Creep under variable stresses is calculated by dividing the stress history

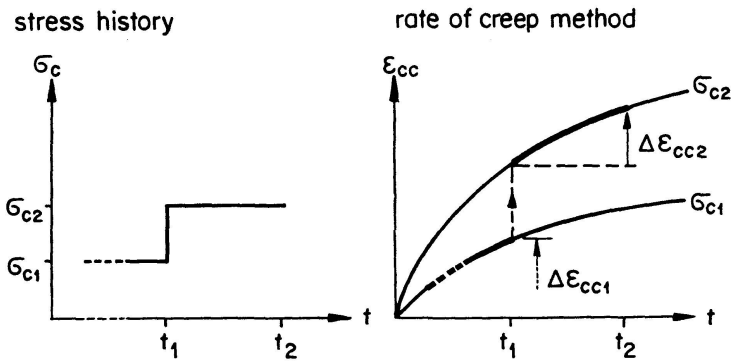Fig. 8. Stress-strain relations.

Fig. 9. Creep under variable stresses.

into time intervals and assuming a constant stress within each interval as indicated in Fig. 9. The "rate of creep" method is applied. It is assumed that the creep under variable stresses can be obtained from creep curves for constant stresses. Such curves, for two stress levels σ_{c1} and σ_{c2}, are indicated with solid lines in Fig. 9. In the time interval $\Delta t = t_2 - t_1$ the increase of strain under the stress σ_{c2} is given by

$$\Delta \, \epsilon_{cc} = \epsilon_0 \, \varphi_\infty \frac{t_1 + \Delta t}{T + t_1 + \Delta t} - \frac{t_1}{T + t_1},\tag{11}$$

where

$$\epsilon_0 = -0.002 \left(1 - \sqrt{1 + \frac{\sigma_{c2}}{f_c}}\right).$$

The procedure for determining the stress σ_{c2} at the end of the time interval $t + \Delta t$ is outlined in Fig. 10. Given are the total strain ϵ at the time $t + \Delta t$, the prior plastic strain ϵ_{cc}, the initial strain ϵ_p and the stress σ_{c1} at the time t. As an approximative solution the stress σ_{c1} is used to determine the increase of creep strain $\Delta \, \epsilon_{cc}$ from Eq. (11). In the case of shrinkage, the corresponding shrinkage strain is added to $\Delta \, \epsilon_{cc}$. The stress σ_{c2} is determined from Eq. (6). If σ_{c2} exceeds the short-time stress corresponding to the total strain ϵ, the latter stress is chosen. The plastic strain ϵ_{cc} at the time $t + \Delta t$ is given by Eq. (7).
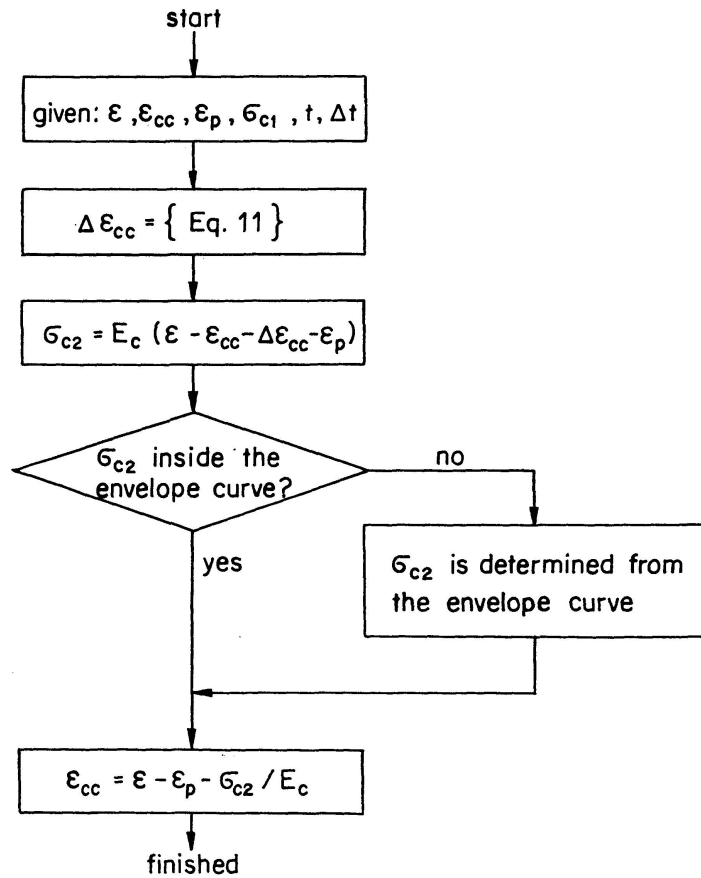

Fig. 10. Determination of stress and "plastic" strain.

4. Computation Procedure

The load carrying capacity of a frame with given cross sections and reinforcements is calculated in successive steps up to the maximum capacity.

Fig. 11 shows the flow-chart used for determining a point on the load-displacement curve. The procedure starts with assumed rigidities for all elements. In a second order elastic analysis, the elastic forces M and N, and the strain distribution expressed by middle strain ϵ_m and curvature $(1/r)$ are determined for all elements. The internal forces M_i and N_i are determined in
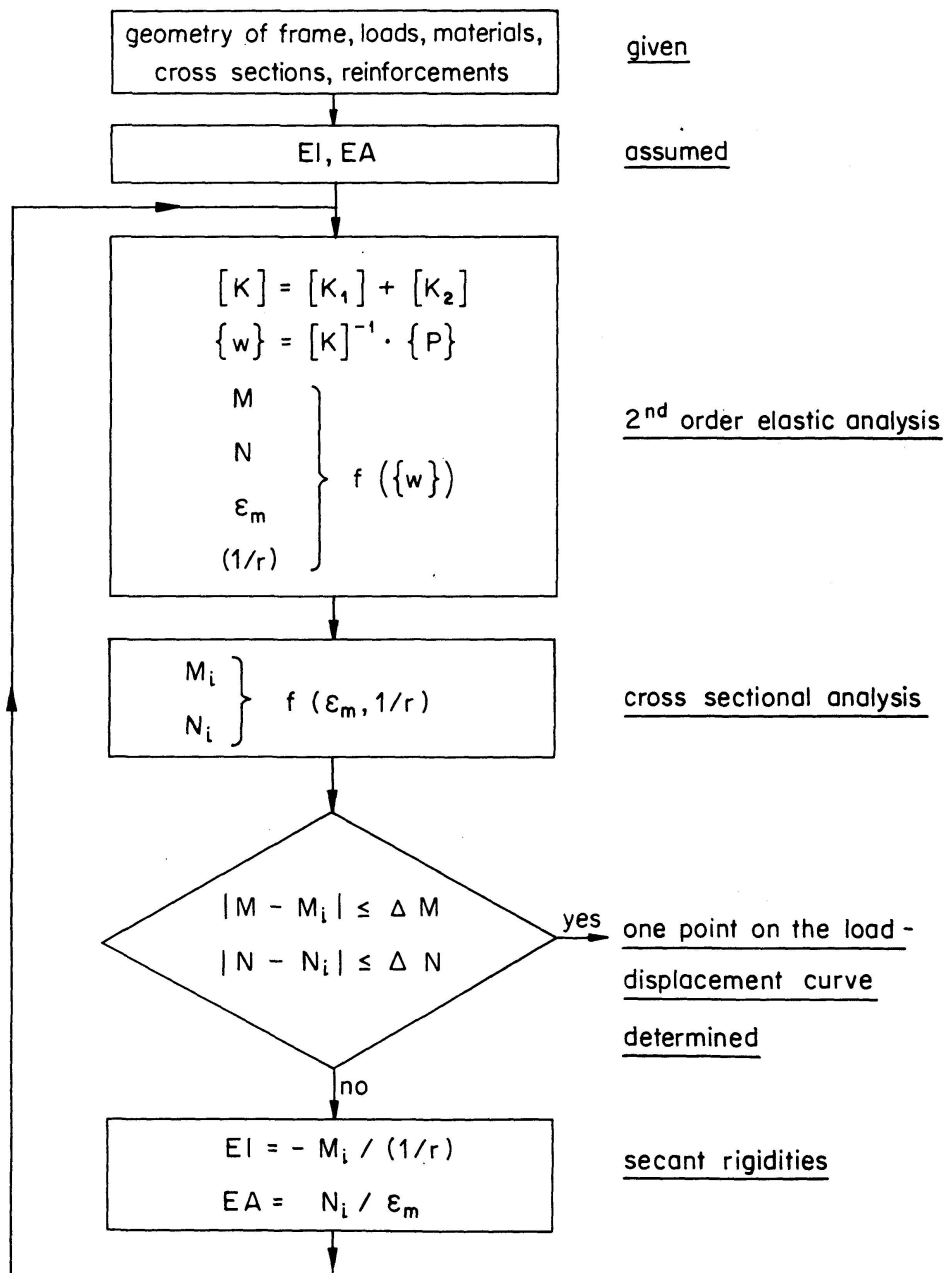

Fig. 11. Flow-chart for frame analysis.

a cross sectional analysis based on the strain distribution found in the elastic analysis. Thus strain equality is automatically satisfied. Force equality then becomes the iteration criterion of the procedure *). If equality is not satisfied, improved secant rigidities are determined from the internal forces, and the procedure is repeated.

The maximum load capacity of slender reinforced concrete frames is associated with instability as indicated in Fig. 12. In a load controlled procedure where the external load is increased in steps poor convergence develops near the maximum load. The unloading part of the curve cannot be calculated. In a displacement controlled procedure, where a characteristic displacement is increased step by step and the corresponding load is calculated, no problems of convergence are encountered.
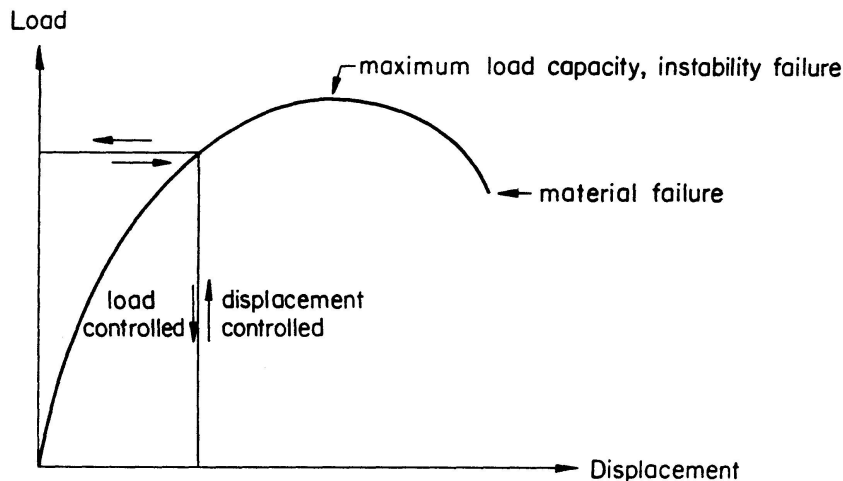

Fig. 12. Load-displacement curve for a slender reinforced concrete frame.

In the present study, external loads on a frame are divided into constant and proportional loads (Fig. 13). The latter are proportional to a load factor λ. A displacement controlled procedure will be used. The displacement w is increased in steps until the maximum value of λ has been found.

For each value of the specified displacement w, the corresponding load factor λ is found iteratively as outlined in the following. First rigidities are assumed for all elements. Then, the load factor λ is increased in steps until calculated and specified displacement coincide. New rigidities can now be determined in the cross sectional analysis. The procedure is repeated until assumed and calculated rigidities agree. The outlined procedure was slightly modified in the above mentioned program in order to speed up the convergence (see Fig. 13). Generally, a non-linear relation exists between the load

*) A slightly different procedure was used in the computer program [1] in order to ensure convergence. In the cross sectional analysis the middle strain ϵ_{mi} was determined iteratively to satisfy the axial force equilibrium. The curvature was kept constant. Moment and middle strain equalities become the iteration criterion in this case.
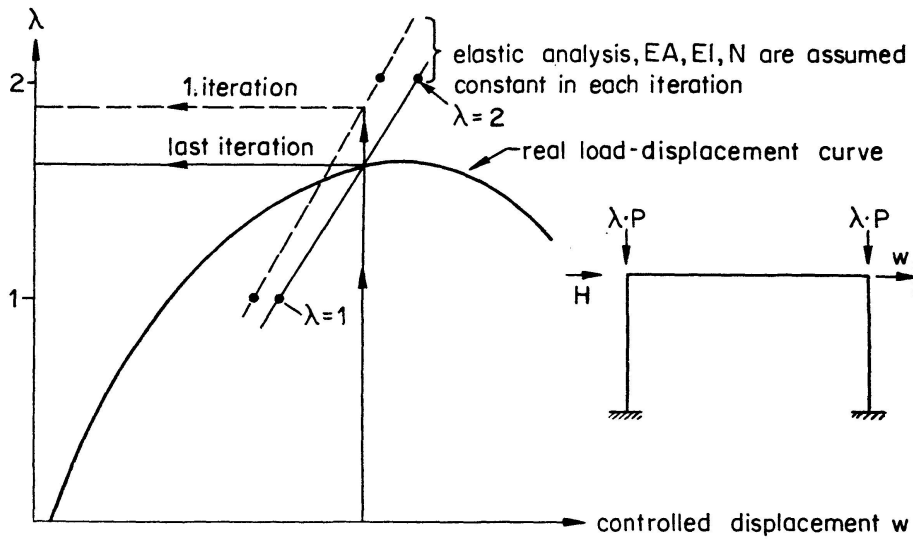
Fig. 13. Displacement controlled determination of a point on the real load-displacement curve.

factor and the displacements even if the rigidities are kept constant. The reason is that the geometrical stiffness matrix $[K_2]$ (Fig. 3) depends on the axial forces N which, in turn, depend on the load factor λ. However, if the axial forces introduced into the geometrical stiffness matrix are assumed independent of λ, a linear relation between λ and the displacement results. Hence, it is sufficient to consider two loading cases, for instance λ equal to 1 and λ equal to 2. The load factor corresponding to the specified displacement w is found by linear interpolation as indicated in Fig. 13. For this new load factor new rigidities and axial forces to be introduced in $[K_2]$ are determined. The procedure is repeated until the calculated rigidities and axial forces agree with the assumed ones.

Under sustained loads, specified by the long-time load factor λ_s and duration t, the displacement w can be calculated as follows:

The displacement w is increased in steps as before. For each step of w, the
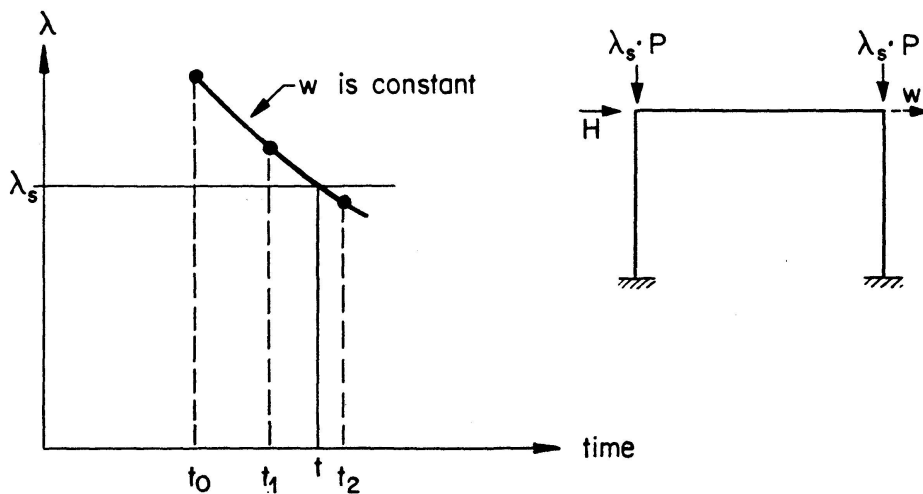

Fig. 14. Displacement controlled[procedure[under[sustained loads.

time is increased in increments. (Fig. 14 corresponds to one value of w; the starting time is t_0.) For each increment of time the corresponding load factor λ is determined as before considering the creep of concrete. When the calculated load factor λ is equal to the given load factor λ_s, the time to reach the chosen displacement has been found. If the calculated λ at the starting time t_0 is less than λ_s, creep instability has taken place.

5. Examples

The following examples illustrate the application of the described analysis.

a) Comparison with Test Results

Three test columns under different types of loads [9] were analysed according to the described method. The three columns had hinged ends on both sides and were of the same length and same cross section (Fig. 15). Due to the symmetry only one half of each column was considered. The column was divided in 6 elements.

Column 24 was loaded in a short time test up to failure (Fig. 15). The measured and the calculated load capacity of 24.2 t agreed favourably. The slightly overestimated middle deflection δ can be explained with the assumption of no tensile strength of the concrete.

Column 25 (Fig. 16) was loaded by a sustained load $P_s = 16.4$ t during 141 days. After this time the increase of deformation was very small. Also for this column the agreement of the measured and computed failure load in the final
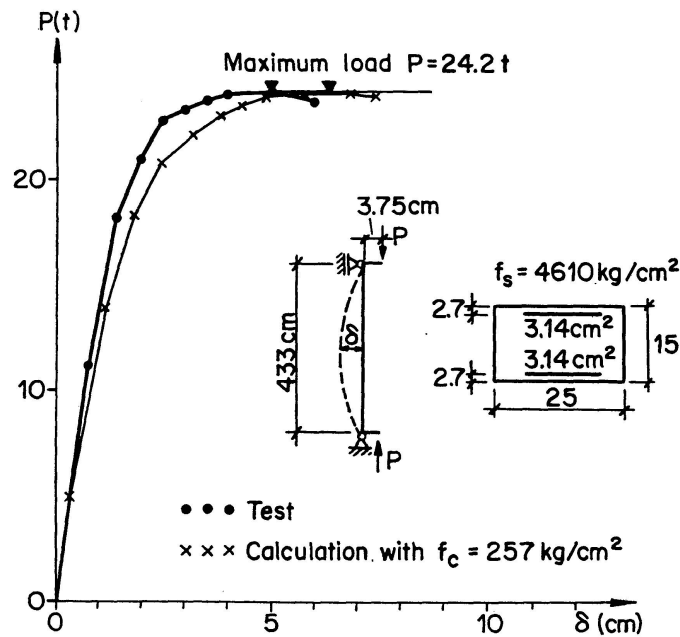

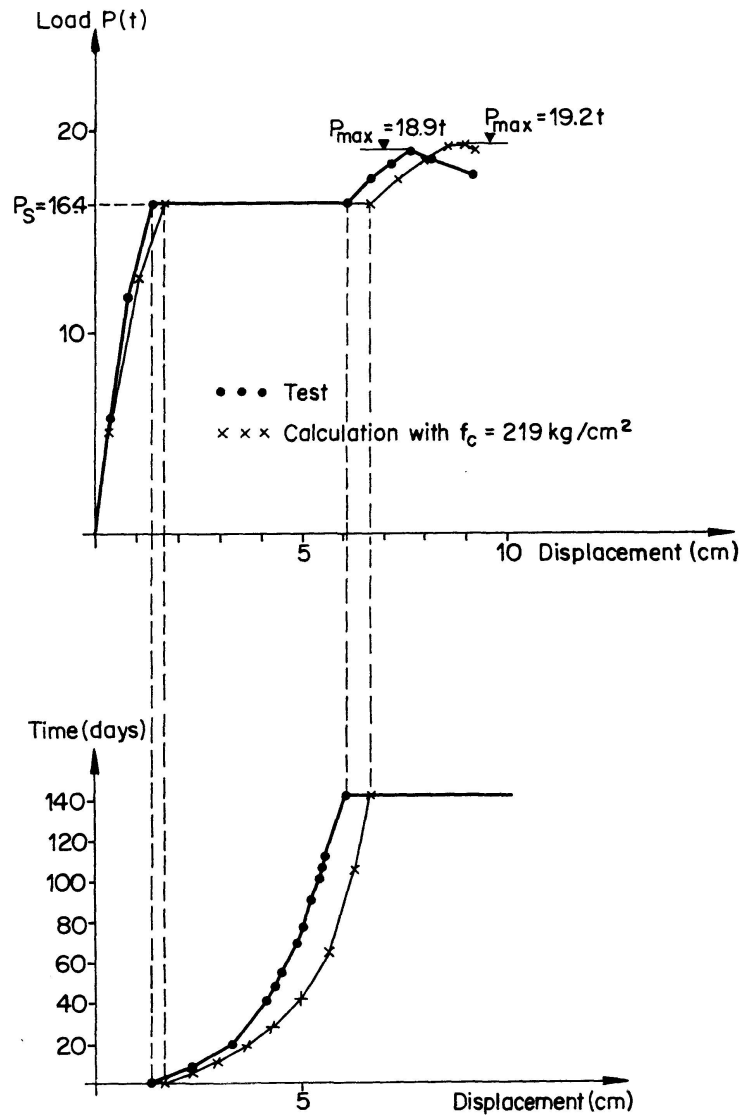Fig. 15. Load-displacement curve (column 24).

Fig. 16. Test under sustained load and final short time test (column 25).

short time test was good ($< 2\%$). The computed deflections both under sustained and under short time loads are too big due to the already mentioned reason. The relation between the middle deflection δ and the time is shown in the lower part of Fig. 16. The agreement of the two curves is satisfactory considering the big scattering which usually is involved in creep problems.

Fig. 17 shows a test under sustained load. The column failed due to creep buckling. The computed load-displacement curve is in good agreement with the measured one. With a middle deflection δ of 9 cm the column becomes unstable under the constant sustained load $P_s = 18.9$ t. The relation between the deflection δ and the time t agrees well up to $t = 61$ days. The computed time at failure is 185 days. The computation of the time depends very much on the assumed concrete strength. To illustrate this the computed time-displacement curve is also given in Fig. 17 for a concrete strength f_c 10% lower than
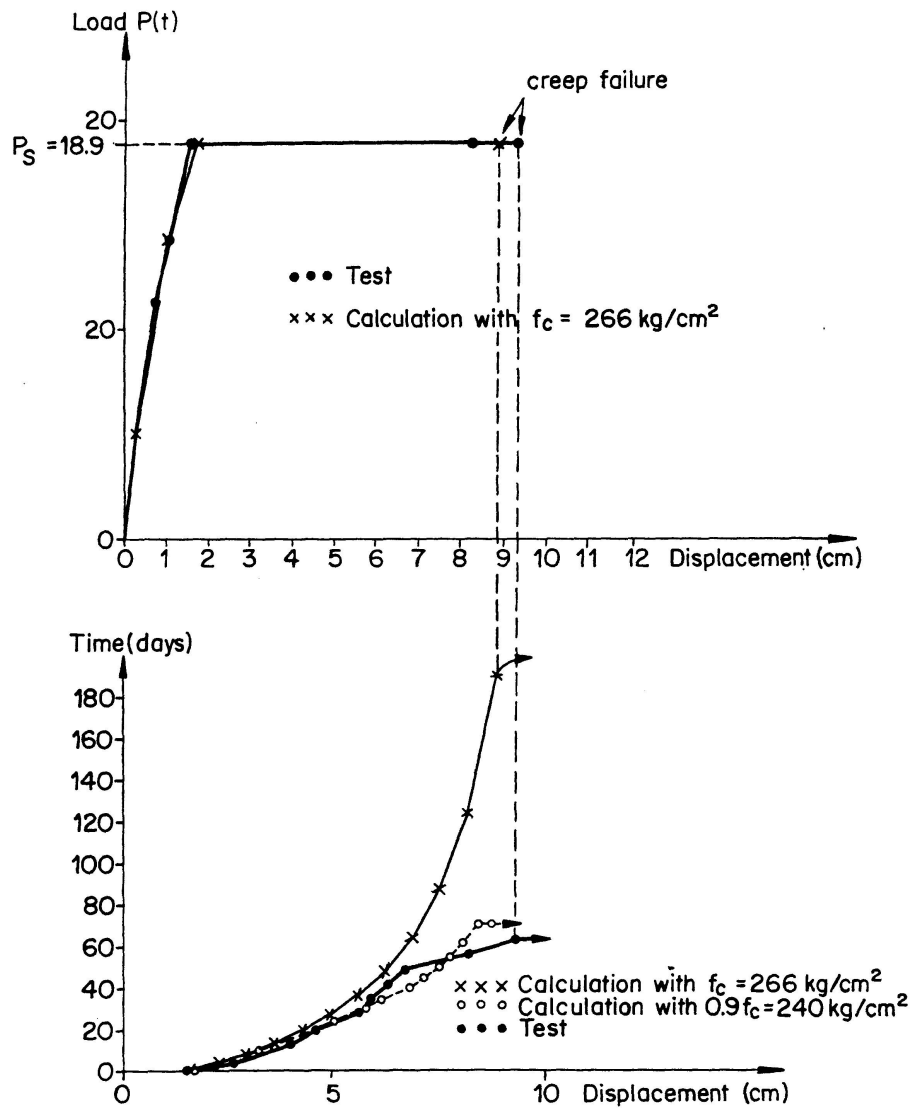
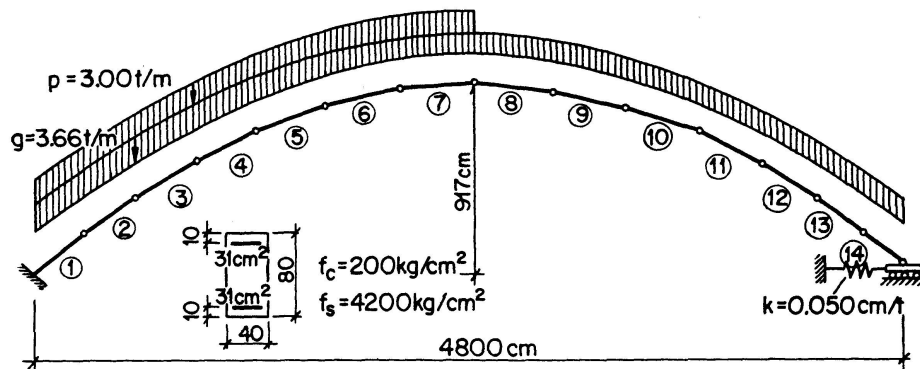Fig. 17. Long time test up to creep failure (column 22).

Fig. 18. System and loads.

the corresponding f_c of the test specimen. In this case the duration of time up to creep failure ($t = 68$ days) is reduced to one third.

b) Arch Under Snow Loads

The arch as shown in Fig. 18 is analysed. As an extreme loading a snow load of $\lambda \cdot 3.00\,\text{t/m}'$ over half the span is assumed for the computation. The dead load $g = 3.66\,\text{t/m}'$ is constant over the whole span. Fig. 19 shows the computed relation between the load factor λ and the maximum deflection at about one third of the span. The dotted line corresponds to a short time loading. In addition to that this relation is also given for a combined short-time and sustained loading. First, the load is increased up to $\lambda = 0.70$ and after a sustained load during 300 days the load is increased up to the maximum load capacity.
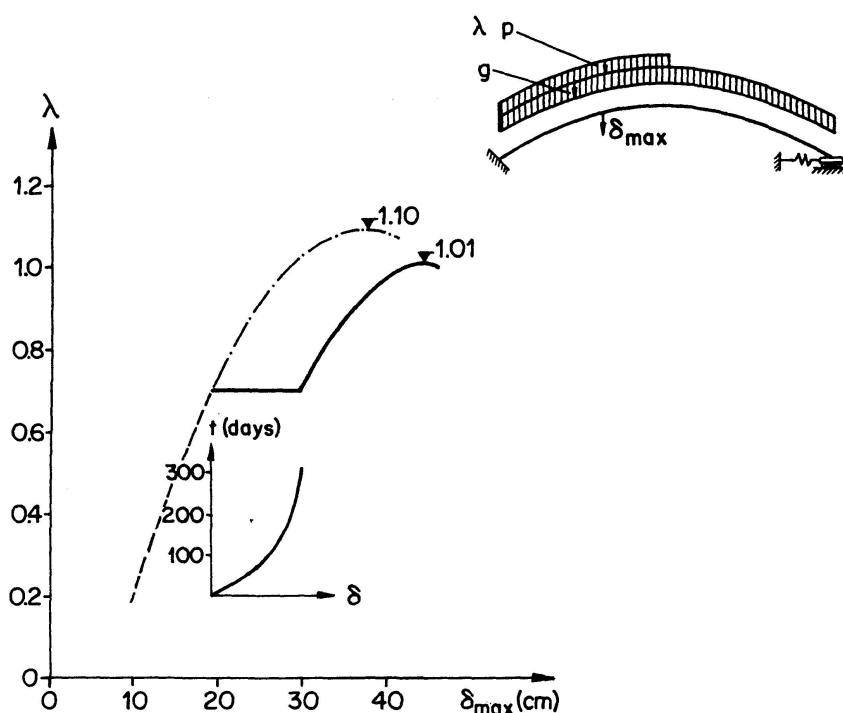
Fig. 19. Load-deflection behavior of an arch under short time and sustained loads.

Notation

M	moment
N	axial force
"i"	subscript "i" is used for reference to the cross sectional analysis
$\{P\}$	external loads
P_s	sustained load
λ	load factor for proportional loads

λ_s	load factor for sustained loads
$[K]$	stiffness matrix
$[K_1]$	first order stiffness matrix
$[K_2]$	non linear geometrical stiffness matrix
$[R]$	transformation matrix
$\{w\}$	nodal displacements
E	modulus of elasticity
A	area of cross section
l	length of element
EI	bending rigidity
EA	axial rigidity
σ	stress
f_s	yiel stress of steel
f_c	cylinder strength of concrete
ϵ	total strain
ϵ_c	"plastic" strain
ϵ_p	initial strain (e. g. due to prestressing)
ϵ_0	short-time strain
φ_∞	limiting creep factor
t	time
T	elapsed time until half of the limiting creep is reached

Acknowledgement

References

1. AAS-JAKOBSEN, K. und GRENACHER, M.: Berechnung unelastischer Rahmen nach der Theorie 2. Ordnung. Bericht Nr. 45, Institut für Baustatik, ETH Zürich.

2. VON KARMAN, T. V.: Untersuchung über Knickfestigkeit. Mitteilung über Forschungsarbeiten auf dem Gebiet des Ingenieurwesens, No. 81, Berlin 1910.

3. BAUMANN, O.: Die Knickung der Eisenbeton-Säulen. Eidg. Materialprüfungsanstalt an der ETH in Zürich. Bericht Nr. 89, Zürich, Dezember 1934.

4. BROMS, B.: Ultimate Strength of Long Reinforced Concrete Columns. Department of Theoretical and Applied Mechanics, University of Illinois, June 1956.

5. PFRANG, E. O. and SIESS, C. P.: Analytical Study of the Behavior of Long Restrained Concrete Columns Subjected to Eccentric Loads. Civil Engineering Studies, Structural Research Series No. 215, University of Illinois, June 1961.

6. BREEN, J. E.: The Restrained Long Concrete Column as a Part of a Rectangular Frame. Ph. D. Dissertation, University of Texas, Austin, Texas, 1962.

7. MANUEL, R. F. and MACGREGOR, J. G.: The Behavior of Restrained Reinforced Concrete Column under Sustained Load. Ph. D. Dissertation, Department of Civil Engineering, The University of Alberta, Canada, 1966.
8. BLAAWENDRAAD, J.: Realistic Analysis of Reinforced Framed Structures. Heron, Vol. 18, No. 4, 1972.
9. RAMU, P., GRENACHER, M., BAUMANN, M., THÜRLIMANN, B.: Versuche an gelenkig gelagerten Stahlbetonstützen unter Dauerlast. Bericht Nr. 6418-1, Institut für Baustatik, ETH Zürich, Mai 1969.

Summary

An approach to analyse reinforced concrete frames is outlined. The effects of second order and non linear material behavior are considered. The computational process described is based on the finite element method. The effective stiffnesses for each state of loading are determined by iteration. The influence of creep and shrinkage are taken into account. Two examples are given to demonstrate the possibilities of the proposed analysis.

Résumé

L'objet de ce rapport est la déscription d'une méthode de calcul selon le 2e ordre pour les structures composées de barres inélastiques. La méthode des éléments finis est à la base de ce calcul. Les rigidités flexionnelles sont calculées pour chaque état de charge par itérations. Les éffets du fluage et du retrait peuvent être considerés. On montre à l'aide de deux exemples les possibilités de cette méthode.

Zusammenfassung

Es wird eine Methode zur Berechnung von Rahmentragwerken aus Stahlbeton beschrieben. Dabei wird der Theorie 2. Ordnung, wie auch dem nicht linearen Materialverhalten, Rechnung getragen. Der beschriebene Rechnungsgang basiert auf der Methode der finiten Elemente. Die effektiven Biegesteifigkeiten für jeden Belastungszustand werden iterativ ermittelt. Langzeiteffekte, wie Kriechen und Schwinden, können berücksichtigt werden. Anhand von zwei Beispielen werden die Möglichkeiten des Rechenverfahrens gezeigt.

Leere Seite

Blank page

Page vide